



## LRP1 activation attenuates white matter injury by modulating microglial polarization through Shc1/PI3K/Akt pathway after subarachnoid hemorrhage in rats



Jianhua Peng<sup>a,b</sup>, Jinwei Pang<sup>a,b</sup>, Lei Huang<sup>b</sup>, Budbazar Enkhjargal<sup>b</sup>, Tongyu Zhang<sup>b</sup>, Jun Mo<sup>b</sup>,  
Pei Wu<sup>b</sup>, Weilin Xu<sup>b</sup>, Yuchun Zuo<sup>b</sup>, Jun Peng<sup>b</sup>, Gang Zuo<sup>b</sup>, Ligang Chen<sup>a</sup>, Jiping Tang<sup>b</sup>,  
John H. Zhang<sup>b,c,d,\*</sup>, Yong Jiang<sup>a,e,f,\*\*</sup>

<sup>a</sup> Department of Neurosurgery, The Affiliated Hospital of Southwest Medical University, Luzhou, Sichuan 646000, China

<sup>b</sup> Department of Physiology and Pharmacology, Loma Linda University, Loma Linda, CA 92350, USA

<sup>c</sup> Department of Anesthesiology, Loma Linda University, Loma Linda, CA 92350, USA

<sup>d</sup> Department of Neurosurgery, Loma Linda University, Loma Linda, CA 92350, USA

<sup>e</sup> Neurosurgery Clinical Medical Research Center of Sichuan Province, Luzhou, Sichuan 646000, China

<sup>f</sup> Nuclear Medicine and Molecular Imaging Key Laboratory of Sichuan Province, Luzhou, Sichuan 646000, China

### ARTICLE INFO

#### Keywords:

Subarachnoid hemorrhage  
White matter injury  
apoE  
LRP1  
Microglia

### ABSTRACT

White matter injury (WMI) is associated with motor deficits and cognitive dysfunctions in subarachnoid hemorrhage (SAH) patients. Therapeutic strategy targeting WMI would likely improve the neurological outcomes after SAH. Low-density lipoprotein receptor-related protein-1 (LRP1), a scavenger receptor of apolipoprotein E (apoE), is able to modulate microglia polarization towards anti-inflammatory M2 phenotypes during inflammation and oxidative insult. In the present study, we investigated the effects of LRP1 activation on WMI and underlying mechanisms of M2 microglial polarization in a rat model of SAH. Two hundred and seventeen male Sprague Dawley rats (weight 280–330 g) were used. SAH was induced by endovascular perforation. LRP1 ligand, apoE-mimic peptide COG1410 was administered intraperitoneally. Microglial depletion kit liposomal clodronate (CLP), LRP1 siRNA or PI3K inhibitor were administered intracerebroventricularly. Post-SAH assessments included neurobehavioral tests, brain water content, immunohistochemistry, Golgi staining, western blot and co-immunoprecipitation. SAH induced WMI shown as the accumulation of amyloid precursor protein and neurofilament heavy polypeptide as well as myelin loss. Microglial depletion by CLP significantly suppressed WMI after SAH. COG1410 reduced brain water content, increased the anti-inflammatory M2 microglial phenotypes, attenuated WMI and improved neurological function after SAH. LRP1 was bound with endogenous apoE and intracellular adaptor protein Shc1. The benefits of COG1410 were reversed by LRP1 siRNA or PI3K inhibitor. LRP1 activation attenuated WMI and improved neurological function by modulating M2 microglial polarization at least in part through Shc1/PI3K/Akt signaling in a rat model of SAH. The apoE-mimic peptide COG1410 may serve as a promising treatment in the management of SAH patients.

### 1. Introduction

Subarachnoid hemorrhage (SAH) accounts for up to 5–7% of all stroke cases with a high mortality rate, as well as leaving 8–20% of its victims in a permanently disabled state [1,2]. Traditional studies focused on the early protection of neuronal cell bodies in cortex or

hippocampus, however, the white matter injury (WMI) is usually neglected. White matter occupies over 50% of the human central nervous system (CNS), which mainly consists of long axons, the ensheathment of axons with myelin and myelin-producing glial cells [3]. White matter has been shown to be more vulnerable to ischemia/hemorrhagic stroke than gray matter and be important cause of cognitive deficits in the

\* Correspondence to: Department of Physiology and Pharmacology, Loma Linda University, School of Medicine, Risley Hall, Room 219, 11041 Campus St, Loma Linda, CA 92354, USA.

\*\* Corresponding author at: Department of Neurosurgery, The Affiliated Hospital of Southwest Medical University, NO.25 of Taiping Street, Luzhou, Sichuan 646000, China.

E-mail addresses: [jhzhang@llu.edu](mailto:jhzhang@llu.edu) (J.H. Zhang), [jiangyong@swmu.edu.cn](mailto:jiangyong@swmu.edu.cn) (Y. Jiang).

<https://doi.org/10.1016/j.redox.2019.101121>

Received 13 December 2018; Received in revised form 18 January 2019; Accepted 22 January 2019

Available online 23 January 2019

2213-2317/ © 2019 The Authors. Published by Elsevier B.V. This is an open access article under the CC BY-NC-ND license (<http://creativecommons.org/licenses/by-nc-nd/4.0/>).

setting of traumatic brain injury (TBI) [4]. In animal models of SAH, there was the presence of WMI in the early stage with characteristics of amyloid precursor protein (APP) accumulation, myelin basic protein (MBP) degradation and white matter edema [5,6]. WMI has also been identified in SAH patients that might be correlated with motor deficits and cognitive dysfunction [7,8]. Thus, therapeutic strategy targeting WMI would likely improve the neurological outcomes after SAH.

We recently demonstrated that a persistent microglia-induced pro-inflammatory microenvironment might be an underlying mechanism that caused WMI after SAH in mice [9]. Depending on the type of stimuli and the pathological conditions, there is a wide range of functional outcomes associated with M1/M2 microglial polarization. While M1 phenotypes of microglia are pro-inflammatory and conducive to the production of reactive oxygen species (ROS), the immunosuppressive M2 microglia phenotypes are phagocytic and anti-inflammatory [10]. A substantial body of evidences has established that the phenotypic shift toward M1 microglia may propel WMI progression after experimental TBI and cerebral ischemia [11,12]. Thus, microglial polarization modulation towards anti-inflammatory, antioxidative M2 phenotype could be in favor of white matter protection after SAH.

Low-density lipoprotein receptor-related protein-1 (LRP1), a scavenger receptor of apolipoprotein E (APOE = gene, apoE = protein), is highly expressed on neurons and glial cells [13]. Previous studies have reported that function of LRP1 in microglia is to keep these cells in an anti-inflammatory and neuroprotective status during inflammatory insult [14]. In the peripheral circulation system, the activation of LRP1/PI3K/Akt signaling prevented macrophage foam cell formation, suppressed inflammation and promoted cell debris clearance [15]. In central nervous system (CNS), Akt appears to play a specific role in modulating microglial M2 polarization via Ser473 phosphorylation after brain injury [12]. Shc1, an evolutionarily conserved adaptor protein, is required for LRP1-dependent signal transduction through PI3K activation and Akt phosphorylation [15].

In the present study, we therefore hypothesized that LRP1-mediated M2 microglial polarization through Shc1/PI3K/Akt pathway would attenuate WMI following SAH in rats.

## 2. Materials and methods

### 2.1. Animals

All procedures in this study were approved by the Institutional Animal Care and Use Committee (IACUC) of Loma Linda University and complied with the National Institutes of Health's Guide for the Care and Use of Laboratory Animals. A total of 217 adult male Sprague Dawley rats (weight 280–330 g, Harlan, Indianapolis, IN, USA) were housed in a vivarium for a minimum of 3 d before surgery with a 12 h light/dark cycle and ad libitum access to food and water.

### 2.2. Experimental design

Total of 5 separate experiments were performed as shown in Fig. 1.

#### 2.2.1. Experiment 1

Characterized the time course of endogenous changes in apoE, LRP1, APP, as well as MBP levels within ipsilateral hemisphere brain tissues at 3 h, 6 h, 12 h, 24 h and 72 h after SAH. Forty-eight rats were randomized into 6 groups: sham ( $n = 6$ ), SAH-3 h ( $n = 7$ ), SAH-6 h ( $n = 6$ ), SAH-12 h ( $n = 7$ ), SAH-24 h ( $n = 14$ ) and SAH-72 h ( $n = 8$ ). Two rats in the SAH-24 h group were used for LRP1 co-localization via immunohistochemistry.

#### 2.2.2. Experiment 2

Evaluated the detrimental role of microglia in WMI at 24 h after SAH. Twenty-eight rats were randomized into the following 3 groups: sham ( $n = 9$ ), SAH + phosphate buffered saline (PBS,  $n = 9$ ) and SAH

+ liposomal clodronate (CLP,  $n = 10$ ). The microglial depletion kit CLP or PBS (FormuMax, Sunnyvale, CA, USA) was injected intracerebroventricularly (i.c.v) using Hamilton syringe (5  $\mu$ l injected in 5 min) at 48 h and 24 h prior to SAH.

#### 2.2.3. Experiment 3 and Experiment 4

Confirmed the beneficial effects of LRP1 activation on neurobehavioral function and WMI. Ninety-nine rats were randomized in the following 5 groups: sham ( $n = 25$ ), SAH + Vehicle (saline) ( $n = 35$ ), SAH + COG1410 (0.2 mg/kg) ( $n = 7$ ), SAH + COG1410 (0.6 mg/kg) ( $n = 26$ ), SAH + COG1410 (1.8 mg/kg) ( $n = 6$ ). The apoE-mimic peptide COG1410 was injected intraperitoneally (i.p.) 30 min after SAH.

#### 2.2.4. Experiment 5

Investigated the underlying mechanism of Shc1/PI3K/Akt pathway in LRP1 mediated microglia polarization modulating. A total of 61 rats were randomized the following 8 groups: naïve + Scramble siRNA ( $n = 3$ ), naïve + LRP1 siRNA ( $n = 3$ ), SAH + Scramble siRNA ( $n = 3$ ), SAH + LRP1 siRNA ( $n = 3$ ), SAH + COG1410 + Scramble siRNA ( $n = 9$ ), SAH + COG1410 + LRP1 siRNA ( $n = 10$ ), SAH + COG1410 + 25% dimethyl sulfoxide (DMSO,  $n = 9$ ), SAH + COG1410 + LY294002 ( $n = 11$ ). Scramble siRNA or LRP1 siRNA (500 pmol in 5  $\mu$ l RNase-free suspension buffer) was injected via i.c.v 48 h before SAH. LY294002 (50 mmol/L, 5  $\mu$ l) or 25% DMSO (5  $\mu$ l) was delivered via i.c.v 30 min before SAH. Western blots were performed using the ipsilateral hemisphere brain tissues collected from all the animals in each group.

### 2.3. SAH model

The endovascular perforation model was induced as previously described [16]. Briefly, rats were intubated and maintained with 3% isoflurane in 70/30% medical air/oxygen by a rodent ventilator (Harvard Apparatus, Holliston, MA, USA). Rodents were placed in a supine position, and the neck was opened with a sharp scalpel in the midline. After localization of the appropriate vessels, a 4–0 nylon suture was inserted into the left internal carotid artery through the external carotid artery stump until resistance was detected. The suture was further advanced 3 mm to perforate the bifurcation of the anterior and middle cerebral artery, followed by immediate withdrawn. In the sham-operated animals, the same procedures were performed without before the vessel perforation. After removal of the suture, the skin incision was closed and the rats were housed individually in heated cages until recovery.

### 2.4. SAH grading

The assessment of SAH grading score was performed at 24 h after SAH by an independent investigator blinded to the experimental group information as previously described [17]. Briefly, basal cisterns were divided into six segments, and each segment was graded from 0 to 3; grades 0, 1, 2, and 3 indicate no obvious subarachnoid blood clot, a minor blood clot, a moderate blood clot, and a large subarachnoid blood clot with an invisible Circle of Willis, respectively. Rats with the grade < 8 at 24 h after SAH were excluded from this study.

### 2.5. Short-term neurological function evaluation

The neurobehavioral function was assessed at 24 h after SAH using modified Garcia and beam balance tests by an investigator blind to experiment as previously described [18]. The modified Garcia test (maximum score = 18) included vibrissae touch, trunk touch, spontaneous activity, spontaneous movement of the four limbs, forelimbs outstretching, and climbing capacity. The beam balance test was conducted to assess the ability of rats to walk on a wooden beam for 1 min.

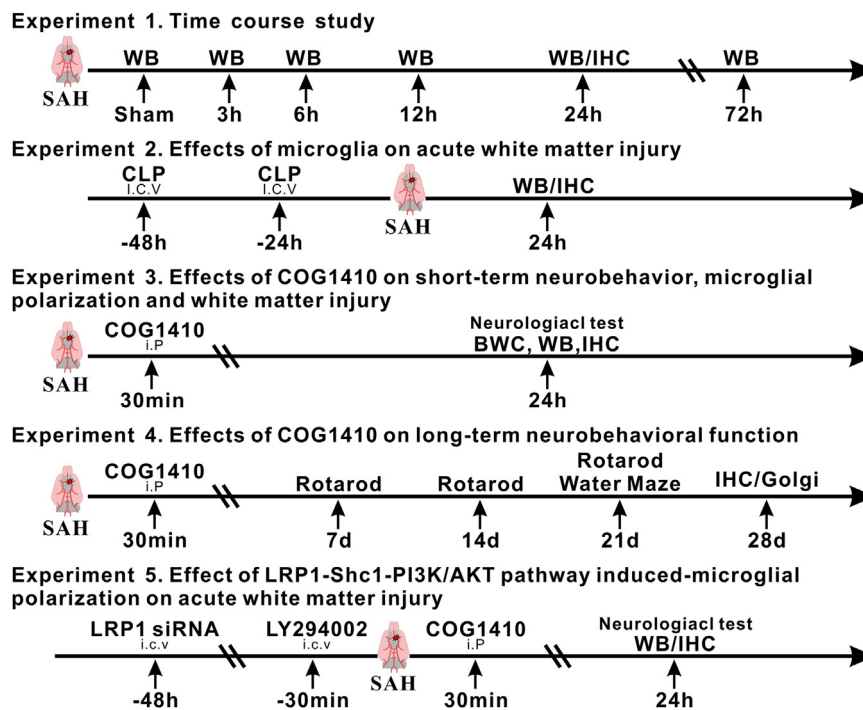


**Fig. 1. Experimental design and animal groups.** SAH, subarachnoid hemorrhage; WB, western blot; IHC, immunohistochemistry; h, hour; CLP, liposomal clonazepam; BWC, brain water content; Golgi, Golgi staining; Scr siRNA, scrambled siRNA; LY294002, PI3K specific inhibitor.

The mean score was calculated based on three consecutive trials scored from 0 to 4 according to the walking ability.

## 2.6. Long-term neurological function evaluation

The rotarod test and Morris water maze were performed evaluate the long-term neurobehavioral function by an investigator blinded to the group information. The rotarod test assessed the motor-sensory deficits as previously described [19]. Briefly, rotarod (Columbus Instruments, Columbus, OH) consists of a rotating horizontal cylinder (7 cm diameter) that is divided into 9.5-cm-wide lanes. Animals had to keep walking forward after being placed on the cylinder. The cylinder started at 5 revolutions per minute (RPM) and 10 RPM, respectively, and accelerated by 2 RPM every 5 s. Latency to fall off was recorded by a photobeam circuit.

The Morris water maze assessed the spatial learning memory and cognitive function as previously described [20]. Briefly, a platform was placed at the center of one of the quadrants. Rats were placed using a semi-random set of start locations to find a visible platform above the water level in 60 s. After that, the rats were guided to the platform and stayed for 5 s. The probe trial was performed at the last day in which the rats were allowed to swim to search the platform submerged in the water. Swim path, swim distance, escape latency, and probe quadrant duration were recorded by a computerized tracking system (Noldus Ethovision; Noldus, Tacoma, WA, USA).

## 2.7. Brain water content

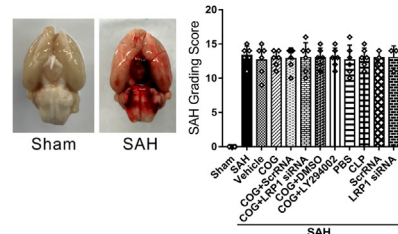
Brain water content was evaluated by a wet/dry method as described previously [21]. Whole brain were harvested at 24 h after SAH and separated into the left hemisphere, right hemisphere, cerebellum, and brain stem. The brain specimens were immediately weighed to obtain the wet weight and then dried at 105 °C for 72 h before determining the dry weight. The percentage of brain water content was calculated as  $[(\text{wet weight} - \text{dry weight})/\text{wet weight}] \times 100\%$ .

## 2.8. Intracerebroventricular administration

Intracerebroventricular drug administration was performed as previously described [21]. Briefly, rats were placed in a stereotaxic apparatus under anesthesia with isoflurane (4% induction, 2.5% maintenance). The needle of a 10- $\mu\text{l}$  Hamilton syringe (Microliter701; Hamilton Company, Reno, NV, USA) was inserted into the right lateral ventricle through a burr hole using the following coordinates relative to bregma: 1.5 mm posterior, 1.0 mm lateral, and 3.2 mm below the horizontal plane of the bregma. For LRP1 in vivo knockdown, a total of 500 pmol LRP1 siRNA duplexes (Thermo Fisher Scientific, Waltham, MA) were dissolved in 5  $\mu\text{l}$  RNase free suspension buffer and then infused into the right lateral ventricle via a pump with the rate 1  $\mu\text{l}/\text{min}$  at 48 h before SAH induction. The same volume of scrambled (Scr) siRNA (Thermo Fisher Scientific, Waltham, MA) was used as a negative control. PI3K-specific inhibitor LY294002 (Selleck Chemicals, Houston, USA) was prepared at 50 mmol/L in PBS (contains 25% DMSO) with a total volume 5  $\mu\text{l}$ . The LY294002 was injected 30 min before SAH. The same volume of 25% DMSO was used as a negative control for LY294002. After injection, the needle was kept in place for an additional 5 min and retracted slowly. Then, the burr hole was sealed with bone wax immediately, and the rats were allowed to recover after sutures.

## 2.9. Western blot

Western blot analysis was performed as previously described [22]. After sample preparation, equal amounts of a sample protein (50  $\mu\text{g}$ ) were loaded onto an SDS-PAGE gel. After electrophoresis, the samples were transferred onto a nitrocellulose membrane. Then, the membrane was blocked for 2 h at room temperature and incubated overnight at 4 °C with the following primary antibodies: anti-apoE (1:500, Abcam, Cambridge, MA, USA), anti-Iba-1 (1:1000, Wako, USA), anti-APP (1:1500, Abcam, Cambridge, MA, USA), anti-myelin basic protein (MBP, 1:1000, Abcam, Cambridge, MA, USA), anti-LRP1 (1:1000, Abcam, Cambridge, MA, USA), anti-Shc1 (1:2000, Abcam, Cambridge, MA, USA), anti-PI3K (1:1000, Cell signaling, USA), anti-Akt (1:1000,

Groups	Mortality Rate	Excluded	Groups	Mortality Rate	Excluded
<b>Experiment 1</b>			<b>Experiment 5.1</b>		
Sham	0(0/6)		SAH+LRP1 siRNA+COG	10%(1/10)	
SAH(3h,6h,12h,24h,72h)	19.05%(8/42)	2	SAH+LRP1 ScrRNA+COG	0(0/9)	
<b>Experiment 2</b>			<b>Experiment 5.2</b>		
Sham*	0(0/9)		naive+ScrRNA	0(0/3)	
SAH+PBS	0(0/9)		naive+LRP1 siRNA	0(0/3)	
SAH+CLP	10%(1/10)		SAH+ScrRNA	0(0/3)	
<b>Experiment 3.1</b>			<b>Experiment 5.2</b>		
Sham	0(0/6)		SAH+LRP1 siRNA	0(0/3)	
SAH+Vehicle	12.50%(1/8)	1	<b>Total</b>		
SAH+COG(0.2mg/kg)	14.29%(1/7)		naive	0(0/6)	
SAH+COG(0.6mg/kg)	0(0/6)		Sham	0(0/31)	
SAH+COG(1.8mg/kg)	0(0/6)		SAH	15%(27/180)	5
<b>Experiment 3.2</b>			<b>*Shared samples with experiment 3</b>		
Sham	0(0/9)				
SAH+Vehicle	16.67%(2/12)	1			
SAH+COG	10%(1/10)				
<b>Experiment 4</b>					
Sham	0(0/10)				
SAH+Vehicle	30%(5/15)				
SAH+COG	30%(3/10)				
<b>Experiment 5.1</b>					
Sham*	0(0/9)				
SAH+Vehicle*	16.67%(2/12)				
SAH+COG*	10%(1/10)				

**Fig. 2. Animal usage and SAH grade.** SAH, subarachnoid hemorrhage; Vehicle, sterile 0.9% of NaCl; COG, COG1410; Scr siRNA, scrambled siRNA; LY294002, PI3K specific inhibitor; DMSO, Dimethyl sulfoxide; PBS, phosphate buffer solution; CLP, clodronate liposomes.

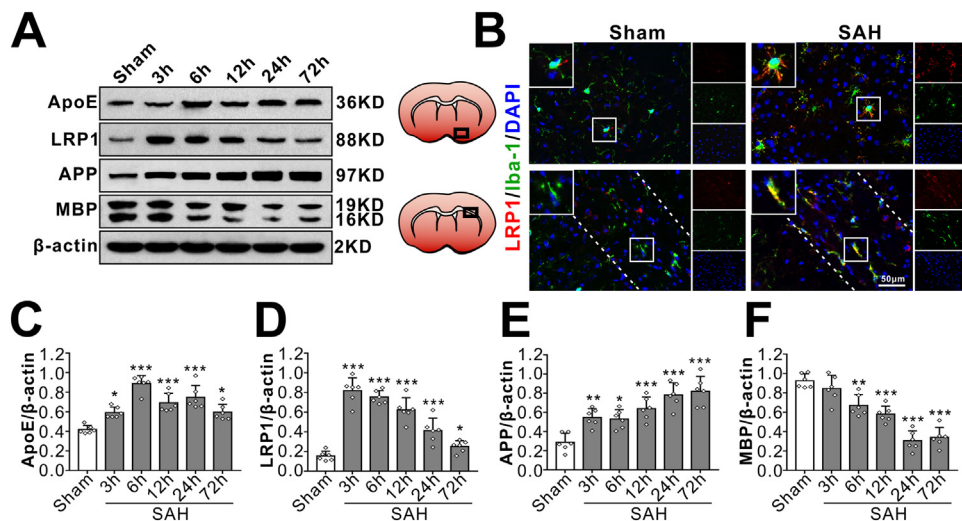


**Fig. 3. Time course of endogenous LRP1 expressions and white matter injury after SAH.** (A, C–F) Representative Western blots band (A) of time course and densitometric quantification of endogenous apoE (C), LRP1 (D), APP (E) and MBP (F) after SAH. \**P* < 0.05, \*\**P* < 0.01, \*\*\**P* < 0.001 vs. Sham group. Data was represented as mean ± SD, n = 6 per group, One-way ANOVA was used followed by Tukey's HSD post hoc test and Holm-Bonferroni correction. (B) Colocalization of LRP1 with microglia in basal cortex (upper panel) and white matter (ipsilateral corpus callosum, lower panel, the dotted line represents the limit of the white matter) at 24 h after sham-operated or SAH. Nuclei are stained with DAPI (blue). Scale bar = 50 μm, n = 3 per group.

Cell signaling, Danvers, MA, USA), anti-phospho-Akt (p-Akt, 1:1000, Cell signaling, Danvers, MA, USA), anti-CD16 (1:1500, Santa Cruz, Dallas, TX, USA), anti-iNOS (1:500, Abcam, Cambridge, MA, USA), anti-CD206 (1:1500, Santa Cruz, Dallas, TX, USA), and anti-β-actin (1:5000, Santa Cruz, Dallas, TX, USA). Appropriate secondary antibodies (1:5000, Santa Cruz, Dallas, TX, USA) were selected to incubate with the membrane for 2 h at room temperature. Then, blot bands were visualized with an ECL reagent (Amersham Biosciences UK Ltd., PA, USA). Non-saturated bands were selected to perform densitometry quantification using Image J software (Image J 1.51, NIH, USA).

**2.10. Immunofluorescence staining**

Double fluorescence staining was performed as described previously [23]. Briefly, the rats were transcardially perfused with ice-cold PBS under deep anesthesia, followed by infusion of 10% paraformaldehyde at 24 h or 28 d after SAH. The whole brains were harvested and then fixed in 10% paraformaldehyde for 24 h followed by 30% sucrose solution until saturation. The brains were cut into 10-μm-thick coronal sections using a cryostat (CM3050S; Leica Microsystems, Bannockburn, III, Germany). The sections were incubated overnight at 4 °C with the

following primary antibodies: anti-ionized calcium-binding adaptor molecule 1 (Iba-1, 1:200, Wako, USA), anti-LRP1 (1:200, Abcam, Cambridge, MA, USA), anti-myelin basic protein (MBP, 1:100, Abcam, Cambridge, MA, USA), anti-amyloid precursor protein (APP, 1:300, Abcam, Cambridge, MA, USA) and anti-neurofilament heavy polypeptide (SMI32, 1:300, Abcam, Cambridge, MA, USA) overnight at 4 °C. After being incubated with the appropriate secondary antibody (1:200, Jackson ImmunoResearch, West Grove, PA, USA) at room temperature for 2 h, the sections were visualized and photographed with a fluorescence microscope (Leica Microsystems, Germany). Microphotographs were analyzed with Image Pro Plus 6.0 software (MediaCybernetics, Bethesda, MD, USA). The numbers of Iba-1-positive cells, APP and SMI32 relative fluorescence intensity were identified and counted in ipsilateral corpus callosum from three random coronal sections per brain.

**2.11. Golgi staining**

The Golgi staining was performed as described previously [24]. Briefly, the rat brain tissues were removed quickly under deep anesthesia on days 28 after SAH. The freshly dissected brains were

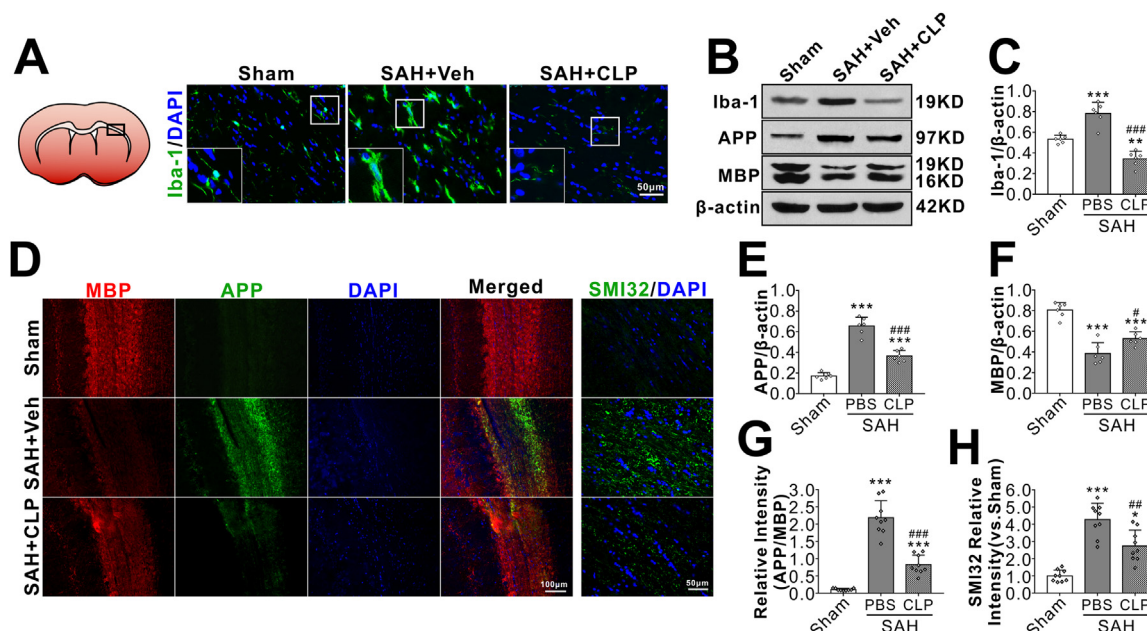


**Fig. 4.** Effects of microglial depletion kit liposomal clodronate (CLP) on white matter injury after SAH. Representative images are shown of immunohistochemistry and western blot assay for microglia marker Iba-1 (A–B), APP and MBP (B). Microglial depletion by CLP (A–C) significantly attenuated the SAH-induced WMI as shown by less APP (B, E) and the greater MBP (B, F) at 24 h after SAH. Compared with the PBS-pretreated SAH, CLP significantly reversed the relative fluorescence intensity of APP (D, G) and SMI32 (D, H). \**P* < 0.05, \*\*\**P* < 0.001 vs. Sham group; #*P* < 0.05, ##*P* < 0.01, ###*P* < 0.001 vs. SAH + PBS group. Data was represented as mean ± SD. One-way ANOVA was used followed by Tukey’s HSD post hoc test and Holm-Bonferroni correction. Western blot, *n* = 6 per group; immunohistochemistry, *n* = 3 per group, regions of interest (ROIs) with white matters were drawn manually on three contiguous slices of each sample. Scale bar = 50 μm or 100 μm.

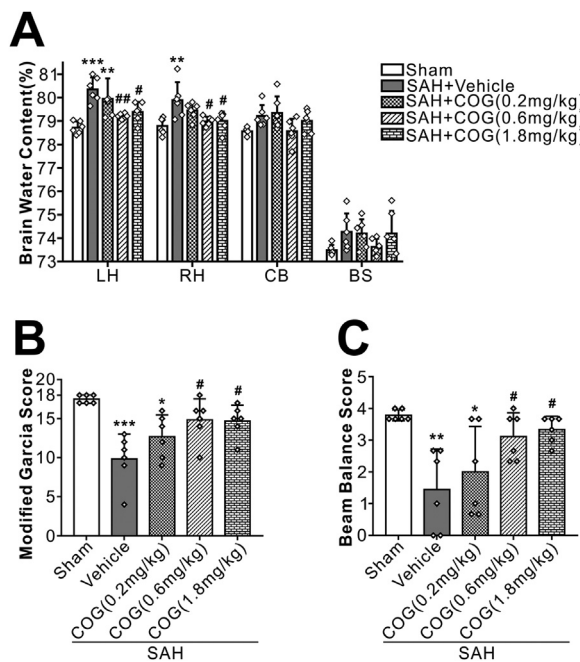


**Fig. 5.** Effects of apoE-mimic peptide COG1410 on neurological functions and brain water content at 24 h after SAH. Treatment with COG1410 reduced brain edema (A) and improved neurological deficits (B, C) at 24 h after SAH (*n* = 6 per group). Data was represented as mean ± SD. One-way ANOVA was used followed by Tukey’s HSD post hoc test and Holm-Bonferroni correction. \**P* < 0.05, \*\**P* < 0.01, \*\*\**P* < 0.001 vs. Sham group; #*P* < 0.05, ##*P* < 0.01, vs. SAH + Vehicle group. Vehicle, sterile 0.9% of NaCl; COG, COG1410.

immersed in solution A and B for 2 weeks at room temperature and transferred into solution C for 72 h at 4 °C. The brains were sliced using a cryostat system (CM3050S; Leica Microsystems, Bannockburn, Ill, Germany) at a thickness of 100 μm. The following staining steps were done according to the FD Rapid GolgiStain™ Kit manufacturer’s protocol (Columbia, USA). Brightfield images for brain samples were taken by Olympus BX51 microscope (Olympus, Waltham, USA). Microphotographs were analyzed with Image Pro Plus 6.0 software (Media Cybernetics, Bethesda, MD, USA).

2.12. Co-immunoprecipitation

To confirm protein-protein binding properties, co-immunoprecipitation (Co-IP) was performed as described previously [15]. Lysates of rat brain tissue were generated under addition of protease inhibitor cocktail and phosphatase inhibitor cocktail (Santa Cruz Biotechnology, Texas, USA). The total protein of the lysates was measured by the Pierce BCA protein assay Kit (Thermo Scientific, Waltham, MA, USA) analyses by a GENESYS 10UV-VIS Spectrophotometer (Thermo Scientific, NY, USA). The rat brain proteins were used for Co-IP experiments performed with the Pierce Co-IP Kit (Thermo Scientific, Waltham, MA, USA). The Co-IP was done according to the manufacturer’s protocol. Ten micrograms of the monoclonal LRP1 (Abcam, Cambridge, MA, USA) were incubated with the delivered resin and covalently coupled. The antibody-coupled resin was incubated with 200 ml of the whole rat testis protein lysates overnight at 4 °C. The resin was washed and the protein complexes bound to the antibody were eluted. Subsequent western blot analyses were performed as described before.

2.13. Statistical analysis

Statistical analysis was performed with Graph Pad Prism (Graph Pad Software, San Diego, CA). All data were expressed as the mean and standard deviation (mean ± SD). One-way analysis of variance

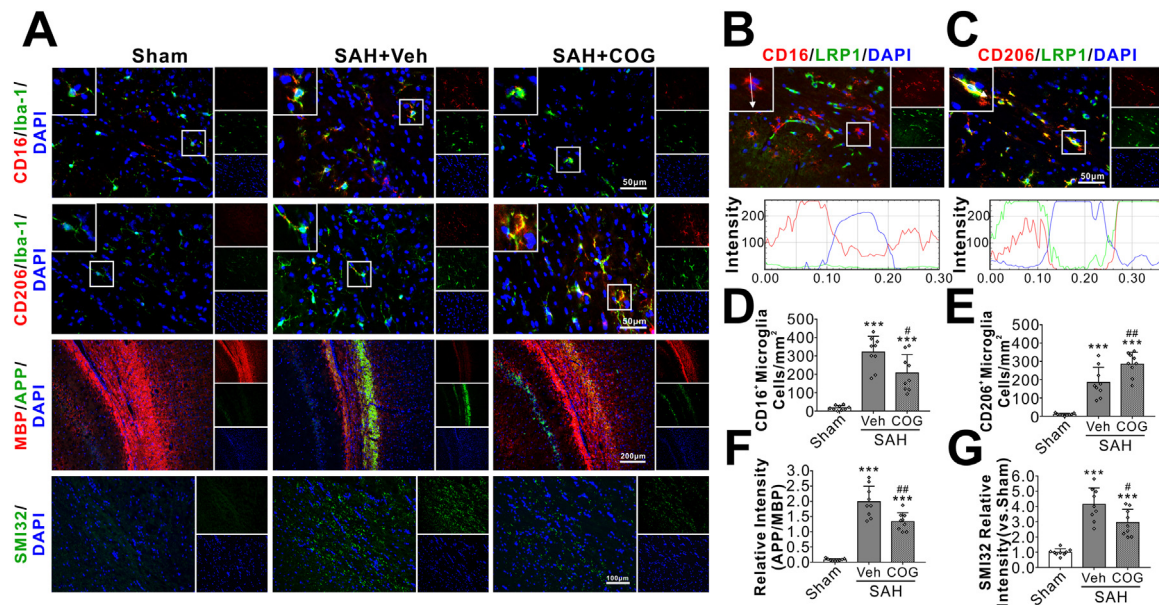


**Fig. 6.** Effects of apoE-mimic peptide COG1410 on microglial polarization and white matter injury at 24 h after SAH. Representative immunohistochemistry microphotographs of microglial polarization and white matter injury staining at 24 h after SAH (A). Immunofluorescent staining against CD16/LRP1 (B) and CD206/LRP1 (C) of the ipsilateral ipsilateral corpus callosum demonstrated that LRP1 was mainly expressed in CD206-positive M2 phenotypes of microglia but not in CD16-positive M1 phenotypes microglia. Treatment with COG1410 reduced CD16-positive M1 phenotypes microglia (D), APP relative intensity (F), SMI32 relative intensity (G), but increased CD206-positive M2 phenotypes of microglia (E). Data was represented as mean  $\pm$  SD. One-way ANOVA was used followed by Tukey's HSD post hoc test and Holm-Bonferroni correction. \*\*\* $P < 0.001$  vs. Sham group; # $P < 0.05$ , ## $P < 0.01$ , vs. SAH + Vehicle group. Vehicle, sterile 0.9% of NaCl; COG, COG1410. Scale bar = 50  $\mu$ m, 100  $\mu$ m or 200  $\mu$ m,  $n = 3$  per group, regions of interest (ROIs) within white matters were drawn manually on three contiguous slices of each sample.

(ANOVA) was used followed by multiple comparisons between groups using Tukey's HSD post hoc test and Holm-Bonferroni correction. Two-way repeated measures ANOVA was used to analyze the long-term neurobehavioral functions over time. A  $P$  value less than 0.05 was considered statistically significant.

### 3. Results

#### 3.1. SAH grade and mortality

There was no significant difference in average SAH grading scores among the SAH groups. All sham-operated rats were survived. The overall mortality of SAH was 15.0%. The mortality was not significantly different among the experimental groups (Fig. 2). Five rats were excluded from this study due to mild SAH (SAH grade < 8).

#### 3.2. Time course of endogenous protein levels of LRP1, apoE and white matter injury markers after SAH

Western blot showed that there were significant increases in LRP1 protein level over 72 h after SAH which peaked at 3 h and decreased gradually during 6–72 h. The endogenous apoE protein level started increasing at 3 h, peaked at 6 h and decreased at 12 h after SAH. APP, a sensitive marker of axonal injury that indicates cytoskeletal damage, showed a continuous elevation over 72 h after SAH that started as early as 3 h. The normal myelin basic protein (MBP) level started decreasing at 6 h and was the lowest at 72 h after SAH (Fig. 3A, C-F). Co-localization of LRP1 with microglia (Iba-1) was observed both in ipsilateral basal cortex and white matter regions (corpus callosum, CC) after SAH (Fig. 3B).

#### 3.3. The effects of microglial depletion on WMI after SAH

In sham rats, immunofluorescence staining showed Iba-1 positive microglia presented the resting morphology with small cell bodies and

thin elongated processes at 24 h after surgery. SAH induced evident microglial activation in brain including white matter regions, manifested as increased cell numbers with morphology of enlarged cell bodies and thick shorter processes. After brain microglia was depleted by i.c.v injection of microglial inhibitor CLP prior to SAH induction, the total numbers of Iba-1 positive microglia in SAH rat was significantly reduced (Fig. 4A). Western blot quantification consistently showed a significantly lower level of Iba-1 protein in SAH + CLP group than that of SAH + vehicle group (Fig. 4B–C). Immunofluorescence (Fig. 4D, G–H) and western blots (Fig. 4B, E–F) showed that axonal injury markers of APP and SMI32 increased and myelin marker MBP decreased at 24 h after SAH. But SAH induced WMI were significantly reversed after microglial depletion by CLP.

#### 3.4. COG1410 ameliorated brain edema and short-term neurobehavioral deficiency after SAH

Twenty-four hours after surgery, SAH animals had significantly higher brain water content in both hemispheres and worse neurobehavioral performances than shams. Compared with animals treated with vehicle, COG1410 at a dose of 0.6 mg/kg and 1.8 mg/kg significantly reduced brain edema (Fig. 5A) and improved the Modified Garcia Score (Fig. 5B) and Beam Balance Score (Fig. 5C). Based on the brain water content and short-term neurobehavioral function results, the dose of 0.6 mg/kg was chosen for the rest of experiments.

#### 3.5. COG1410 attenuated WMI by modulating microglial polarization after SAH

SAH significantly increased the total numbers of Iba-1 positive microglia at 24 h after injury, in which CD16 positive M1 phenotypes predominated over CD206 positive M2 phenotypes. COG1410 treatment significantly decreased the M1 phenotypes but increased the M2 phenotypes of activated microglia (Fig. 6A, D–E). Double immunofluorescence staining showed that LRP1 was mainly expressed in

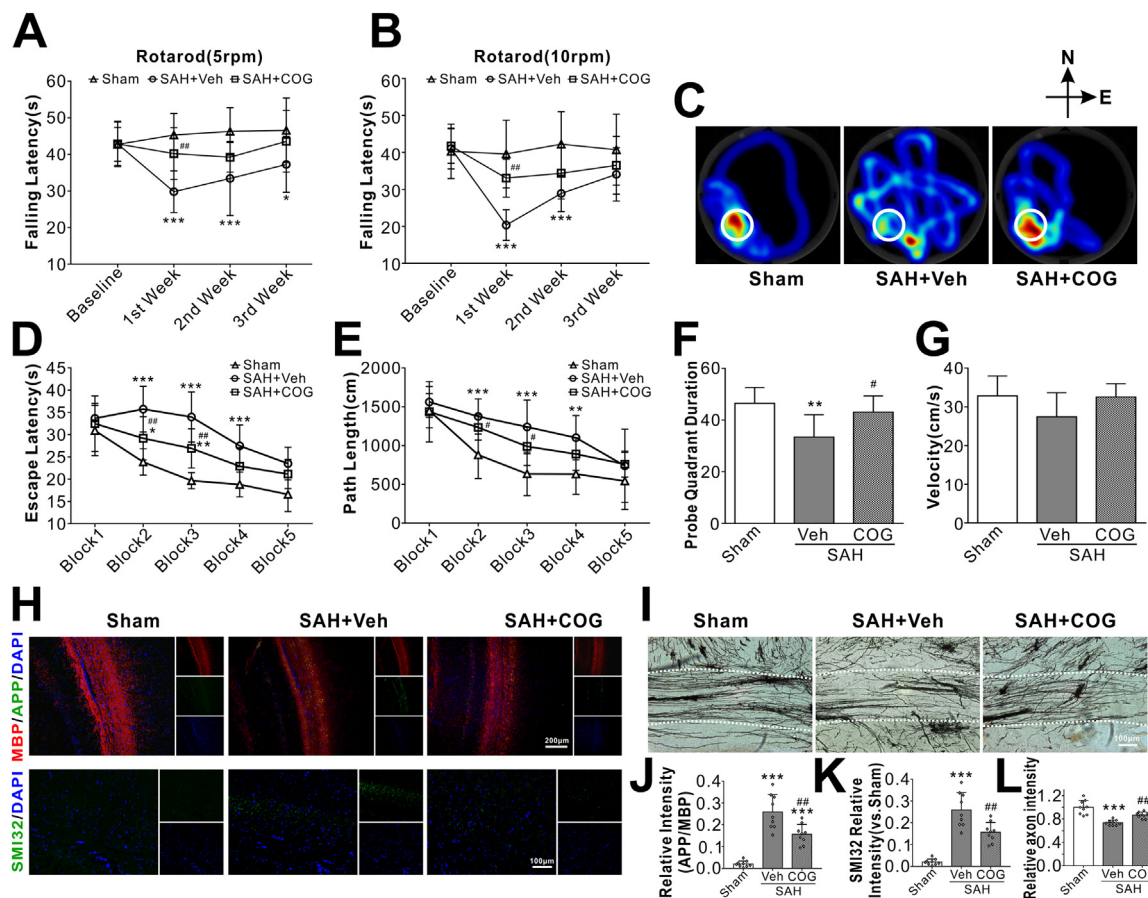


**Fig. 7.** Effect of apoE-mimic peptide COG1410 on long-term neurological function at 28 d after SAH. (A, B) Rotarod tests of 5 RPM and 10 RPM. (C) Representative heatmaps of the probe trial. The white circles indicate the positions of the probe platform. (D, E) Escape latency and swimming distance of Morris Water Maze. (F) Quantification of the probe quadrant duration in the probe trial. (G) Swimming velocities of different groups in probe trial. Representative microphotographs of immunohistochemistry staining (H) and quantitative analysis of APP (J), SMI32 (K) were performed within ipsilateral white matters. Representative microphotographs of Golgi staining (I) and quantitative analysis for axons (L) were performed within ipsilateral white matters. Data was represented as mean  $\pm$  SD (n = 7–10 per group). \*P < 0.05, \*\*P < 0.01, \*\*\*P < 0.001 vs. Sham group; #P < 0.05, ##P < 0.01, vs. SAH + Vehicle group. Vehicle, sterile 0.9% of NaCl; COG, COG1410.

CD206-positive M2 phenotypes but not in CD16-positive M1 phenotypes of activated microglia (Fig. 6B–C). Associated with the microglial M1 to M2 phenotypic shift, the axonal injury markers of APP and SMI32 were significantly attenuated by COG1410 treatment at 24 h after SAH (Fig. 6A, F–G).

### 3.6. COG1410 improved long-term neurobehavioral outcome after SAH

SAH rats showed significantly shorter falling latency in both 5 RPM and 10 RPM rotarod tests compared with the shams on days 7 and 14 after SAH. However, the administration of COG1410 significantly improved the rotarod performance in SAH rats (Fig. 7A–B). In the water maze test, the travel distance and escape latency for the rats to find the platform were significantly increased in the SAH + vehicle group compared with the sham group. However, a significantly shorter time and swim distance to find the platform were observed on block 2 and block 3 in the SAH + COG1410 group (Fig. 7D–E). In probe quadrant trial, the rats in the SAH + vehicle group spent remarkably less time in the target quadrant when compared with sham group, while the reference memory deficits were significantly improved by COG1410 treatment (Fig. 7C, F). There was no significant difference in swimming velocity among all three groups (Fig. 7G). The immunofluorescence staining could still detect the expressions of APP and SMI32 at 28 d after SAH, which was significantly decreased by COG1410 treatment (Fig. 7H, J–K). Furthermore, Golgi staining showed that the broken

axons in the SAH + vehicle group that were better preserved in the SAH + COG1410 group (Fig. 7I, L).

### 3.7. LRP1 siRNA and LY294002 reversed the effects of COG1410 on microglial polarization and WMI at 24 h after SAH

Injection of LRP1 siRNA via i.c.v 48 h before SAH induction significantly decreased the expression of LRP1 both in naïve and SAH rats, which confirmed the knockdown efficacy of LRP1 siRNA in the present study (Fig. 8A, B). Although COG1410 treatment had no effect on LRP1 expression after SAH, it significantly increased the protein levels of Shc1, PI3K, phosphorylated-Akt (Ser473), microglia M2 phenotype marker CD206 and myelin marker MAP but decreased protein levels of M1 phenotype marker CD 16 and iNOS, axonal injury marker APP when compared with vehicle treated SAH rats. When the LRP1 expression was knockdown in the SAH + COG1410 + LRP1 siRNA group, the effects of COG1410 on Shc1/PI3K/Akt signaling pathway activation, M2 microglial polarization and white matter protection were reversed when compared with the SAH + COG1410 + Scr siRNA group (Fig. 8C–L).

The PI3K inhibitor LY294002 was used to assess PI3K involvement in the signaling pathway underlying the effects of LRP1-mediated microglial polarization and sequent WMI attenuation after SAH. Without changes of LRP1 and Sch1 protein levels, pretreatment with PI3K inhibitor LY294002 significantly reversed COG1410 effects on the expressions of PI3K, phosphorylated-Akt (Ser473), M2 microglial

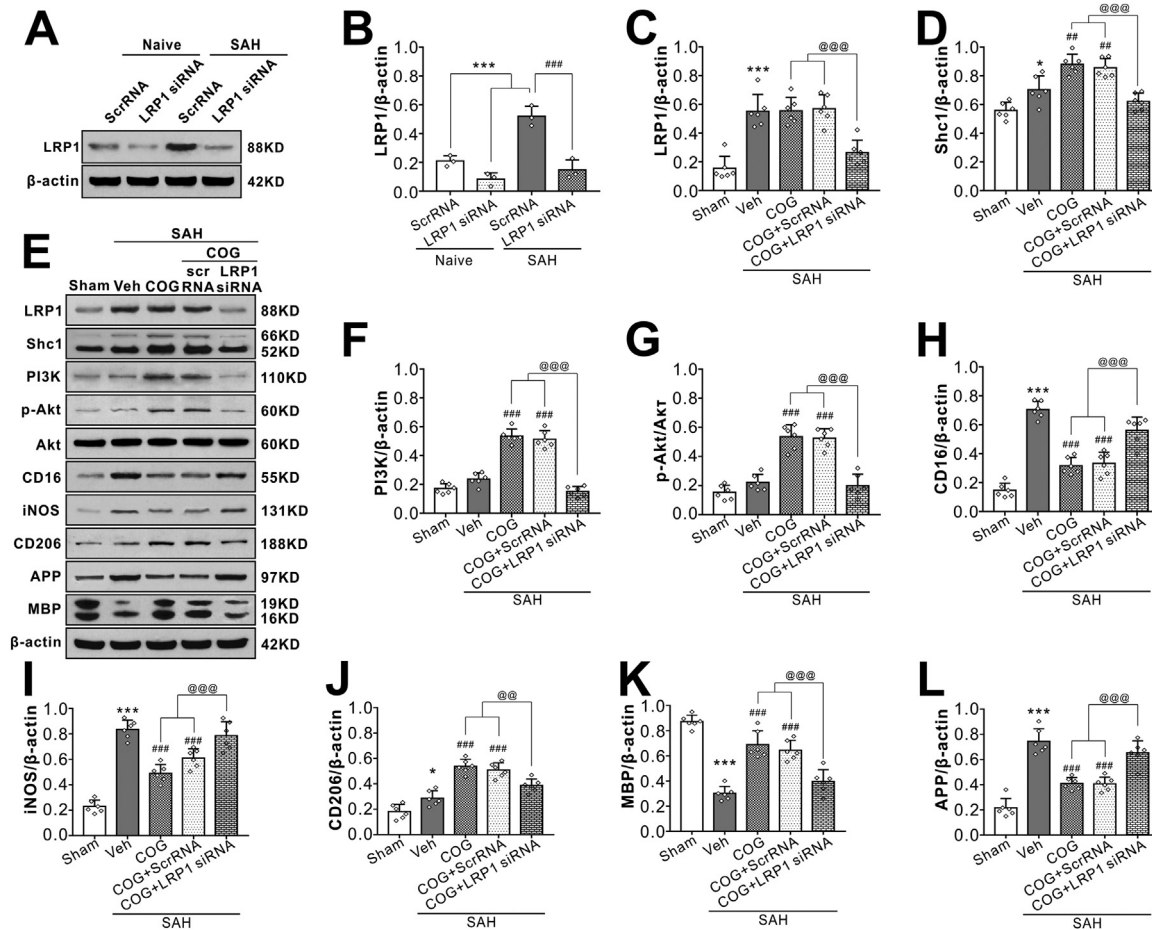


**Fig. 8.** LRP1-knockout abolished the beneficial effect of COG1410 on M2 microglia polarization, white matter protection at 24 h after SAH. (A–B) LRP1-knockout efficiency evaluation. LRP1 siRNA significantly decreased LRP1 protein expression both in normal rats and SAH rats. Data was represented as mean ± SD (n = 3 per group). One-way ANOVA was used followed by Tukey’s HSD post hoc test and Holm-Bonferroni correction. \*\*\*P < 0.001 vs. Naive + ScrRNA group; ###P < 0.001 vs. SAH + ScrRNA group; (C–L) Representative western blot bands and quantification of LRP1, Shc1, PI3K, p-Akt/Akt, CD16, iNOS, CD206, APP, and MBP. Data was represented as mean ± SD (n = 6 per group). One-way ANOVA was used followed by Tukey’s HSD post hoc test and Holm-Bonferroni correction. \*P < 0.05, \*\*\*P < 0.001 vs. Sham group; ###P < 0.01, ###P < 0.001 vs. SAH + Vehicle group; @P < 0.01, @@@P < 0.001 vs. SAH + COG + LRP1 siRNA group. Vehicle, sterile 0.9% of NaCl; COG, COG1410; ScrRNA, scrambled siRNA.

phenotype marker CD206, M1 microglial phenotype marker CD 16, myelin marker MAP and axonal injury marker APP in the SAH + COG1410 + LY294002 group when compared with the SAH + COG1410 + DMSO group at 24 h after SAH (Fig. 9A–G, I–K).

### 3.8. Interaction of LRP1 with apoE and the intracellular adaptor protein Shc1

Using co-immunoprecipitation, we observed the binding endogenous ligand apoE and intracellular adaptor protein Shc1 to LRP1 in the sham or SAH rats brain tissues. As shown in Fig. 9H, apoE and Shc1 were co-immunoprecipitated with LRP1 both in sham and SAH group at 24 h after surgery, which providing a direct evidence of the interaction of LRP1 with its ligand apoE and intracellular adaptor protein Shc1. Furthermore, our results showed that the interaction of endogenous apoE with LRP1 and Shc1 with LRP1 were increased in the SAH brain tissue compared with that of sham group.

## 4. Discussion

In the present study, we made the following novel findings: (1) endogenous apoE and its binding receptor LRP1 were significantly increased over 72 h after SAH which peaked at 6 h and 3 h, respectively. LRP1 were co-localized with microglia within whiter matter regions.

While the white matter axonal injury marker APP was increased, the normal myelin marker MBP was decreased continually over 72 h starting at 3 h after SAH; (2) the depletion of microglia by CLP prior to SAH induction significantly attenuated WMI at 24 h after SAH; (3) intraperitoneal injection of an apoE-mimic peptide COG1410 30 min after SAH significantly decreased brain water content at 24 h after SAH, improved neurobehavioral deficits at 24 h and 28 d after SAH; (4) COG1410 treatment attenuated WMI at 24 h and 28 d after SAH by modulating microglial polarization towards to CD206 positive M2 phenotypes; (5) COG1410 treatment significantly up-regulated the expression of intracellular adaptor protein Shc1, PI3K, p-Akt, M2 microglial phenotype marker CD206 and normal myelin marker MBP but decreased M1 microglial phenotype markers and axonal injury marker APP at 24 h after SAH. LRP1 mainly expressed in CD206 positive M2 microglia but less in CD16 positive M1 microglia. LRP1 siRNA and specific PI3K inhibitor LY294002 significantly reversed the aforementioned COG1410 effects on WMI, M2 microglial polarization and Shc1/PI3K/Akt activation; (6) LRP1 was directly bound to endogenous apoE ligand and intracellular adaptor protein Shc1 in rats brain tissue at 24 h after SAH. The results suggested that the activation of Shc1/PI3K/Akt signaling pathway possibly underlined the effects of COG1410 in the LRP1 mediated microglial polarization modulation.

White matter comprises over 50% of the human CNS and the two major constituents, namely axons and myelin, are remarkably



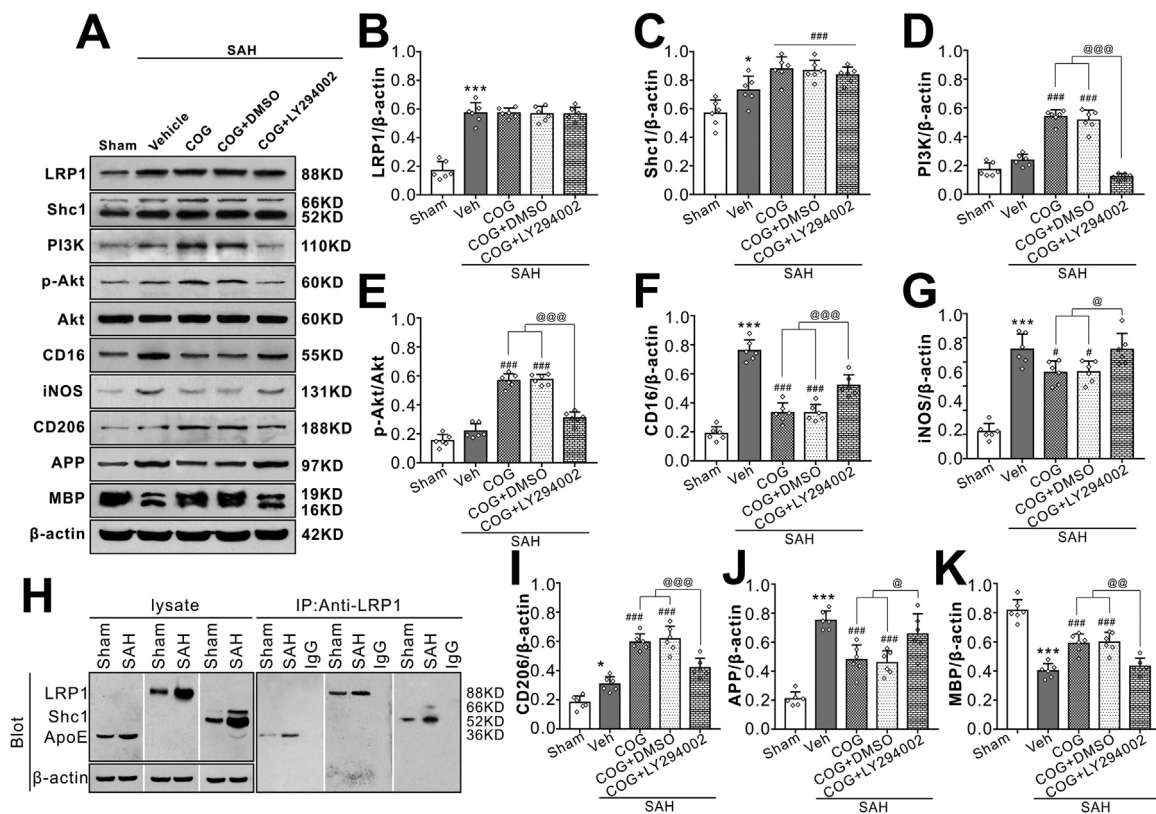


**Fig. 9. Inhibition of PI3K abolished the beneficial effect of COG1410 on M2 microglia polarization, white matter protection at 24 h after SAH. (AG, I–K)** Representative western blot bands and quantification of LRP1, Shc1, PI3K, p-Akt/Akt, CD16, iNOS, CD206, APP, and MBP. Data was represented as mean ± SD (n = 6 per group). (H) LRP1 was binding to endogenous apoE and Shc1 in brain tissue from Sham or SAH rats. One-way ANOVA was used followed by Tukey’s HSD post hoc test and Holm-Bonferroni correction. \**P* < 0.05, \*\*\**P* < 0.001 vs. Sham group; ###*P* < 0.001 vs. SAH + Vehicle group; @*P* < 0.05, @@*P* < 0.01, @@@*P* < 0.001 vs. SAH + COG + LY294002 group. Vehicle, sterile 0.9% of NaCl; COG, COG1410; DMSO, Dimethyl sulfoxide, LY294002, PI3K inhibitor.

vulnerable to pressure, ischemia and inflammation [25,26]. The sudden increase in intracranial pressure (ICP) and blood content in the sub-arachnoid space are two major causes of acute brain injury after SAH. We previously demonstrated that arterial rupture could induce a sharp elevation in ICP, which might impose the mechanical pressure on axons [27]. Other events such as blood–brain barrier disruption or heme iron overload attributed to the WMI after SAH [5,28]. Importantly, we recently found that WMI in SAH showed obvious regional distribution characteristics that mainly presented within the regions with glial cell aggregation. A recent study demonstrated that inhibition of glial inflammatory and oxidative response could improve cognition and motor complications [29]. Thus pro-inflammatory and pro-oxidative micro-environment associated with microglial activations may be critical for WMI progression in the settings of SAH [9]. Consistently, our current study showed that there were significantly increased axonal injury marker APP and decreased normal myelin marker MBP over the 72 h after SAH, indicating WMI. Microglial depletion by CLP pretreatment significantly suppressed the WMI at 24 h after SAH, characterized by better preservation of normal myelin marker MBP and less axonal injury markers of APP and SMI32. In spite of its significant benefits on WMI reduction in the early phase post experimental SAH, complete microglial depletion, however, may not represent a reasonable therapeutic strategy to be applied in the clinical setting.

Upon stimulation and activation, microglial polarized to M1 or M2 phenotypes with distinct functions of pro-inflammatory and immunosuppressive, respectively [30]. Microglial polarization to M1 phenotypes contributed to white matter damage and selectively activated microglial M2 phenotypes helped tissue repairing under conditions of acute brain injury including ischemic stroke [31], traumatic brain injury [12] and spinal cord injury [32]. In experimental SAH

animals and clinical SAH patients, the activated microglia has been reported to act as double-edge sword, which could either protect against neuronal cell death and cerebral blood toxicity or impair cognitive function [33]. Thus, therapies that prime microglia towards the anti-inflammatory M2 phenotype may offer new therapeutic targets to attenuate WMI in the setting of SAH. Our data demonstrated that a BBB permeable apoE-mimic peptide COG1410 promoted M2 microglial polarization through LRP1 activation, leading to less brain edema and WMI as well as neurological deficits in a rat model of SAH.

Emerging data supports the multiple neuroprotective properties of apoE including anti-inflammation [34], anti-apoptosis [35], anti-oxidant [36] and cerebrovascular integrity maintainability [37]. In humans, apoE is the major apolipoprotein expressed in the brain and exists as three isoforms, designated E2, E3, and E4. Many studies, including our previous clinical research, have demonstrated that the presence of the APOEε4 allele predisposes patients to clinical deterioration [27,38,39]. Importantly, Bell et al. showed that glial-secreted apoE3 and murine apoE, but not apoE4, could signal to surrounding cells via LRP1 [13]. COG1410 is a peptide derive from apoE amino acid residues 138–149 of the receptor region of apoE holoprotein with aminoisobutyric acid (Aib) substitutions at positions 140 and 145 (acetyl-AS-Aib-LRKL-Aib-KRLL-amide), which does not include the polymorphic residues at positions 112 and 158 that define the E2, E3, and E4 isoforms of apoE in humans [40]. Our data indicated that COG1410 promoted M2 microglial polarization after SAH. Specifically, apoE has been shown to play a crucial role in macrophage conversion from pro-inflammatory M1 to anti-inflammatory M2 phenotype [41]. Furthermore, we have recently revealed the involvement of apoE in the process of microglial polarization post SAH [42]. However, how apoE and COG1410 affect microglial polarization remains elusive.

In the present study, the Co-IP results indicated direct protein-protein binding effects of apoE with its receptor LRP1. As a receptor for free heme, hemopexin (Hx) and the Hx-heme complex, LRP1 acts as heme scavenger and signaling receptor transports of multiple binding partners [43]. In humans, LRP1 is a major amyloid- $\beta$  (A $\beta$ ) clearance receptor contributes to A $\beta$  clearance [44]. We confirmed the presence of LRP1 in microglia using immunohistochemistry and noticed an increased expression of brain LRP1 after SAH. LRP1 knockdown with LRP1 siRNA significantly abolished the treatment effects of apoE-mimic peptide COG1410 on M2 microglial polarization. The decreased expression in pro-inflammatory/pro-oxidative M1 microglia marker and increased expression in anti-inflammatory M2 microglia marker CD206 suggested a positive feedback loop involving LRP1 activation and M2 microglial polarization. Furthermore, we observed that LRP1 was mainly expressed in CD206-positive M2 microglia but less in CD16-positive M1 microglia. Congruently, previous study showed that microglia deficient in LRP1 adopted a pro-inflammatory phenotype and exhibited the microglia morphological observed under inflammatory conditions [14]. Thus, the function of LRP1 in microglia is likely to keep these cells in an anti-inflammatory and neuroprotective status during inflammatory insult after SAH.

Our Co-IP results also showed that LRP1 directly bind to the intracellular adaptor protein Shc1. As an evolutionarily conserved adaptor protein that mediates inflammation signaling, Shc1 is required for LRP1-dependent signal transduction through activation of PI3K and phosphorylation of Akt [15]. Under conditions involving injury, Akt regulated M2 microglial polarization via Ser473 phosphorylation [12]. Our data showed that LRP1 knockdown by siRNA or PI3K inhibition by the specific inhibitor LY294002 significantly reversed the M2 microglial polarization effects of apoE-mimic peptide COG1410. These data suggested the apoE-mimic peptide COG1410 promoted M2 microglial polarization by activating Shc1/PI3K/Akt pathway through LRP1 after SAH in rats.

There are several limitations in this study. First, LRP1 plays multifunctional roles in lipid homeostasis, signaling transduction, and endocytosis [45]. Further research is needed to investigate the other mechanisms underlying the neuroprotective effects of LRP1 against WMI after SAH. Second, this study focused on the LRP1 mediated M2 microglial polarization on white matter protection after SAH. We could not exclude the neurological benefits of LRP1 activation were the results of both gray and white matter protections. Detailed roles of LRP1 on CNS cells, such as neurons, astrocytes, endothelial cells and oligodendrocytes are necessary for further study. Third, apoE has been shown to be bound and internalized via receptor-mediated endocytosis by other receptors, including the low-density lipoprotein receptor (LDLR), very-low density lipoprotein receptor (VLDLR) and apoE receptor 2 (apoEr2) in the CNS [46], further studies are needed to understand how apoE-mimic peptide COG1410 affects these receptors and the related pathways.

In conclusion, we demonstrated that LRP1 activation by apoE-mimic peptide COG1410 attenuated WMI and improved neurological function by modulating microglial polarization toward M2 phenotypes after SAH. This regulation was at least in part through Shc1/PI3K/Akt signaling. Thus apoE-mimic peptide COG1410 may serve as a promising treatment in the management of SAH patients.

## Acknowledgments

This work was supported by the National Institutes of Health (NS081740, NS082184, NS081740 and NS082184), the National Natural Science Foundation of China (81771278 and 81801176) and the Technology Innovation Talent Project of Sichuan Province (2018RZ0090, 19MZGC0003).

## Declaration of interest

The authors declare that they have no conflict of interest.

## References

- [1] M.T. Lawton, G.E. Vates, Subarachnoid hemorrhage, *N. Engl. J. Med.* 377 (2017) 257–266.
- [2] D.J. Nieuwkamp, L.E. Setz, A. Algra, et al., Changes in case fatality of aneurysmal subarachnoid haemorrhage over time, according to age, sex, and region: a meta-analysis, *Lancet Neurol.* 8 (2009) 635–642.
- [3] R.F. Fern, C. Matute, P.K. Stys, White matter injury: ischemic and nonischemic, *Glia* 62 (2014) 1780–1789.
- [4] Z. Kou, P.J. VandeVord, Traumatic white matter injury and glial activation: from basic science to clinics, *Glia* 62 (2014) 1831–1855.
- [5] Y. Egashira, H. Zhao, Y. Hua, et al., White matter injury after subarachnoid hemorrhage: role of blood-brain barrier disruption and matrix metalloproteinase-9, *Stroke* 46 (2015) 2909–2915.
- [6] T.T. Kummer, S. Magnoni, C.L. MacDonald, et al., Experimental subarachnoid haemorrhage results in multifocal axonal injury, *Brain* 138 (2015) 2608–2618.
- [7] R. Darwazeh, M. Wei, J. Zhong, et al., Significant injury of the mammillothalamic tract without injury of the corticospinal tract after aneurysmal subarachnoid hemorrhage: a retrospective diffusion tensor imaging study, *World Neurosurg.* 114 (2018) e624–e630.
- [8] S.S. Yeo, B.Y. Choi, C.H. Chang, et al., Evidence of corticospinal tract injury at midbrain in patients with subarachnoid hemorrhage, *Stroke* 43 (2012) 2239–2241.
- [9] Y. Wu, J. Peng, J. Pang, et al., Potential mechanisms of white matter injury in the acute phase of experimental subarachnoid haemorrhage, *Brain* 140 (2017) e36.
- [10] Z. Yu, D. Sun, J. Feng, et al., MSX3 switches microglia polarization and protects from inflammation-induced demyelination, *J. Neurosci.* 35 (2015) 6350–6365.
- [11] X. Hu, P. Li, Y. Guo, et al., Microglia/macrophage polarization dynamics reveal novel mechanism of injury expansion after focal cerebral ischemia, *Stroke* 43 (2012) 3063–3070.
- [12] G. Wang, Y. Shi, X. Jiang, et al., HDAC inhibition prevents white matter injury by modulating microglia/macrophage polarization through the GSK3 $\beta$ /PTEN/Akt axis, *Proc. Natl. Acad. Sci. USA* 112 (2015) 2853–2858.
- [13] R.D. Bell, E.A. Winkler, I. Singh, et al., Apolipoprotein E controls cerebrovascular integrity via cyclophilin A, *Nature* 485 (2012) 512–516.
- [14] T.Y. Chuang, Y. Guo, S.M. Seki, et al., LRP1 expression in microglia is protective during CNS autoimmunity, *Acta Neuropathol. Commun.* 4 (2016) 68.
- [15] X. Xian, Y. Ding, M. Dieckmann, et al., LRP1 integrates murine macrophage cholesterol homeostasis and inflammatory responses in atherosclerosis, *Elife* 6 (2017).
- [16] K. Duris, J. Lipkova, Z. Splichal, et al., Early inflammatory response in the brain and anesthesia recovery time evaluation after experimental subarachnoid hemorrhage, *Transl. Stroke Res.* (2018).
- [17] L. Shi, A. Al-Baadani, K. Zhou, et al., PCMT1 ameliorates neuronal apoptosis by inhibiting the activation of MST1 after subarachnoid hemorrhage in rats, *Transl. Stroke Res.* (2017).
- [18] W. Wan, Y. Ding, Z. Xie, et al., PDGFR- $\beta$  modulates vascular smooth muscle cell phenotype via IRF-9/SIRT-1/NF- $\kappa$ B pathway in subarachnoid hemorrhage rats, *J. Cereb. Blood Flow Metab.* (2018) (271678X18760954).
- [19] Z. Xie, B. Enkhjargal, L. Wu, et al., Exendin-4 attenuates neuronal death via GLP-1R/PI3K/Akt pathway in early brain injury after subarachnoid hemorrhage in rats, *Neuropharmacology* 128 (2017) 142–151.
- [20] Q. Zhu, B. Enkhjargal, L. Huang, et al., Aggf1 attenuates neuroinflammation and BBB disruption via PI3K/Akt/NF- $\kappa$ B pathway after subarachnoid hemorrhage in rats, *J. Neuroinflamm.* 15 (2018) 178.
- [21] L. Huang, P. Sherchan, Y. Wang, et al., Phosphoinositide 3-kinase gamma contributes to neuroinflammation in a rat model of surgical brain injury, *J. Neurosci.* 35 (2015) 10390–10401.
- [22] Y. Wu, J. Pang, J. Peng, et al., An apoE-derived mimic peptide, COG1410, alleviates early brain injury via reducing apoptosis and neuroinflammation in a mouse model of subarachnoid hemorrhage, *Neurosci. Lett.* 627 (2016) 92–99.
- [23] J. Mo, B. Enkhjargal, Z.D. Travis, et al., AVE 0991 attenuates oxidative stress and neuronal apoptosis via Mas/PKA/CREB/UCP-2 pathway after subarachnoid hemorrhage in rats, *Redox Biol.* 20 (2018) 75–86.
- [24] S. Zagout, A.M. Kaindl, Golgi-cox staining step by step, *Front. Neuroanat.* 10 (2016) 38.
- [25] E.T. Mandeville, C. Ayata, Y. Zheng, et al., Translational MR neuroimaging of stroke and recovery, *Transl. Stroke Res.* 8 (2017) 22–32.
- [26] Y. Wang, G. Liu, D. Hong, et al., White matter injury in ischemic stroke, *Prog. Neurobiol.* 141 (2016) 45–60.
- [27] J. Peng, X. Qin, J. Pang, et al., Apolipoprotein Epsilon4: a possible risk factor of intracranial pressure and white matter perfusion in good-grade aneurysmal subarachnoid hemorrhage patients at early stage, *Front. Neurol.* 8 (2017) 150.
- [28] Y. Egashira, Y. Hua, R.F. Keep, et al., Lipocalin 2 and blood-brain barrier disruption in white matter after experimental subarachnoid hemorrhage, *Acta Neurochir. Suppl.* 121 (2016) 131–134.
- [29] A.I. Rojo, M. Pajares, A.J. Garcia-Yague, et al., Deficiency in the transcription factor NRF2 worsens inflammatory parameters in a mouse model with combined tauopathy and amyloidopathy, *Redox Biol.* 18 (2018) 173–180.
- [30] X. Hu, R.K. Leak, Y. Shi, et al., Microglial and macrophage polarization – new prospects for brain repair, *Nat. Rev. Neurol.* 11 (2015) 56–64.
- [31] C. Qin, W.H. Fan, Q. Liu, et al., Fingolimod protects against ischemic white matter

- damage by modulating microglia toward M2 polarization via STAT3 pathway, *Stroke* 48 (2017) 3336–3346.
- [32] D.P. Stirling, K. Cummins, M. Mishra, et al., Toll-like receptor 2-mediated alternative activation of microglia is protective after spinal cord injury, *Brain* 137 (2014) 707–723.
- [33] N. Schallner, R. Pandit, R. LeBlanc 3rd et al., Microglia regulate blood clearance in subarachnoid hemorrhage by heme oxygenase-1, *J. Clin. Invest.* 125 (2015) 2609–2625.
- [34] V. Theendakara, C.A. Peters-Libeu, P. Spilman, et al., Direct transcriptional effects of apolipoprotein E, *J. Neurosci.* 36 (2016) 685–700.
- [35] J.T. Yu, L. Tan, J. Hardy, Apolipoprotein E in Alzheimer's disease: an update, *Annu. Rev. Neurosci.* 37 (2014) 79–100.
- [36] M. Rosenblat, N. Volkova, R. Coleman, et al., Anti-oxidant and anti-atherogenic properties of liposomal glutathione: studies in vitro, and in the atherosclerotic apolipoprotein E-deficient mice, *Atherosclerosis* 195 (2007) e61–e68.
- [37] J. Pang, Y. Chen, L. Kuai, et al., Inhibition of blood-brain barrier disruption by an apolipoprotein E-mimetic peptide ameliorates early brain injury in experimental subarachnoid hemorrhage, *Transl. Stroke Res.* 8 (2017) 257–272.
- [38] H.T. Wu, J. Ruan, X.D. Zhang, et al., Association of promoter polymorphism of apolipoprotein E gene with cerebral vasospasm after spontaneous SAH, *Brain Res.* 1362 (2010) 112–116.
- [39] H.M. Wilkins, S.J. Koppel, R. Bothwell, et al., Platelet cytochrome oxidase and citrate synthase activities in APOE epsilon4 carrier and non-carrier Alzheimer's disease patients, *Redox Biol.* 12 (2017) 828–832.
- [40] X. Qin, H. You, F. Cao, et al., Apolipoprotein E mimetic peptide increases cerebral glucose uptake by reducing blood-brain barrier disruption after controlled cortical impact in mice: an 18F-fluorodeoxyglucose PET/CT study, *J. Neurotrauma* 34 (2017) 943–951.
- [41] D. Baitsch, H.H. Bock, T. Engel, et al., Apolipoprotein E induces antiinflammatory phenotype in macrophages, *Arterioscler. Thromb. Vasc. Biol.* 31 (2011) 1160–1168.
- [42] J. Pang, J. Peng, N. Matei, et al., Apolipoprotein E exerts a whole-brain protective property by promoting M1? Microglia quiescence after experimental subarachnoid hemorrhage in mice, *Transl. Stroke Res.* 9 (2018) 654–668.
- [43] G. Wang, A. Manaenko, A. Shao, et al., Low-density lipoprotein receptor-related protein-1 facilitates heme scavenging after intracerebral hemorrhage in mice, *J. Cereb. Blood Flow Metab.* 37 (2017) 1299–1310.
- [44] T. Kanekiyo, C.C. Liu, M. Shinohara, et al., LRP1 in brain vascular smooth muscle cells mediates local clearance of Alzheimer's amyloid-beta, *J. Neurosci.* 32 (2012) 16458–16465.
- [45] A.P. Lillis, L.B. Van Duyn, J.E. Murphy-Ullrich, et al., LDL receptor-related protein 1: unique tissue-specific functions revealed by selective gene knockout studies, *Physiol. Rev.* 88 (2008) 887–918.
- [46] Y.A. Huang, B. Zhou, M. Wernig, et al., ApoE2, ApoE3, and ApoE4 differentially stimulate APP transcription and abeta secretion, *Cell* 168 (2017) 427–441 (e421).